NEUROSCIENCE
RESEARCH ARTICLE
M. L. Rossi et al. / Neuroscience 385 (2018) 198–214

Pre- and Postsynaptic Effects of Glutamate in the Frog Labyrinth

Maria Lisa Rossi, [a]* **Gemma Rubbini,** [a] **Marta Martini,** [a] **Rita Canella** [a] **and Riccardo Fesce** [b]

[a] *Dipartimento di Scienze della Vita e Biotecnologie, Ferrara University, Ferrara, Italy*

[b] *Centre of Neuroscience, DISTA, Insubria University, Varese, Italy*

Abstract—The role of glutamate in quantal release at the cytoneural junction was examined by measuring mEPSPs and afferent spikes at the posterior canal in the intact frog labyrinth. Release was enhanced by exogenous glutamate, or DL-TBOA, a blocker of glutamate reuptake. Conversely, drugs acting on ionotropic glutamate receptors did not affect release; the α-amino-3-hydroxy-5-methyl-4-isoxazolepropionic acid receptor (AMPA-R) blocker CNQX decreased mEPSP size in a dose-dependent manner; the NMDA-R blocker D-AP5 at concentrations <200 μM did not affect mEPSP size, either in the presence or absence of Mg and glycine. In isolated hair cells, glutamate did not modify Ca currents. Instead, it systematically reduced the compound delayed potassium current, IKD, whereas the metabotropic glutamate receptor (mGluR)-II inverse agonist, (2*S*)-2-amino-2-[(1*S*,2*S*)-2-carboxycycloprop-1-yl]-3-(xanth-9-yl)propanoic acid (LY341495), increased it. Given mGluR-II decrease cAMP production, these finding are consistent with the reported sensitivity of IKD to protein kinase A (PKA)-mediated phosphorylation. LY341495 also enhanced transmitter release, presumably through phosphorylation-mediated facilitation of the release machinery. The observed enhancement of release by glutamate confirms previous literature data, and can be attributed to activation of mGluR-I that promotes Ca release from intracellular stores. Glutamate-induced reduction in the repolarizing IKD may contribute to facilitation of release. Overall, glutamate exerts both a positive feedback action on mGluR-I, through activation of the phospholipase C (PLC)/IP_3 path, and the negative feedback, by interfering with substrate phosphorylation through $G_{i/0}$-coupled mGluRs-II/III. The positive feedback prevails, which may explain the increase in overall rates of release observed during mechanical stimulation (symmetrical in the excitatory and inhibitory directions). The negative feedback may protect the junction from over-activation.

Key words: isolated frog labyrinth, synaptic transmission, sensory discharge, glutamate, GluR and mGluR, Hair cell calcium and potassium currents.

INTRODUCTION

A number of studies have strongly suggested that glutamate is the afferent transmitter at the cytoneural junction in the inner ear of several animal species (Raymond et al., 1988; see Guth et al., 1998a; Ottersen et al., 1998; Usami et al., 2001 for reviews). In the vestibular system, the role of glutamate in the afferent synaptic transmission has been widely described in the cat (Dechesne et al., 1984), turtle (Bonsacquet et al., 2006; Holt et al., 2006, 2007), guinea pig (Demêmes et al., 1995; Devau et al., 1993), rat (Safieddine and Wenthold, 1997; Lysakowski et al., 2011; Sadeghi et al., 2014) and frog labyrinth (Annoni et al., 1984; Prigioni et al., 1994; Prigioni and Russo, 1995; Guth et al., 1998a,b; Hendricson and Guth, 2002a,b). In the crista ampullaris of frog semicircular canals, only type II hair cells are present, which are believed to release glutamate on postsynaptic ionotropic glutamate receptors (α-amino-3-hydroxy-5-methyl-4-isoxazolepropionic acid receptor (AMPA)) located on the bouton endings of afferent fibers.

Metabotropic glutamate receptors (mGluRs) group I are involved in cochlear function (Niedzielski et al., 1997; Kleinlogel et al., 1999). As regards the vestibular

*Corresponding author. Address: Dipartimento di Scienze della Vita e Biotecnologie, Via Borsari 46, 44121 Ferrara, Italy.
E-mail address: rsm@unife.it (M. L. Rossi).

Abbreviations: Glu, L-glutamic acid monosodium salt monohydrate; DMSO, dimethyl sulphoxide; mEPSP, miniature excitatory postsynaptic potential; ICa, calcium current; IKD, delayed potassium current; PKA, protein kinase A; ER, endoplasmic reticulum; LY341495, (2*S*)-2-amino-2-[(1*S*,2*S*)-2-carboxycycloprop-1-yl]-3-(xanth-9-yl)propanoic acid; LY379268, (1*R*,4*R*,5*S*,6*R*)-4-amino-2-oxabicyclo[3.1.0]hexane-4,6-dicarboxylic acid; DL-TBOA, DL-threo-β-benzyloxyaspartic acid; AMPAR, α-amino-3-hydroxy-5-methyl-4-isoxazolepropionic acid receptor; Glycine CNQX, 6-cyano-7-nitroquinoxaline-2,3-dione disodium salt hydrate; D-AP5, D-(−)-2-amino-5-phosphonovaleric acid; GLAST, (EAAT1), excitatory amino acid transporter I; NMDA, N-methyl-D-aspartic acid; mGluR, metabotropic glutamate receptor; ACPD, ±1-aminocyclopentane-trans-1,3-dicarboxylate; 4-CPG, (*S*)-4-carboxyphenylglycine; AIDA, (*RS*)-1-aminoindan-1,5-dicarboxylic acid; DHPG, (*RS*)-3,5-dihydroxyphenylglycine hydrate; 2APB, 2-aminoethoxydiphenyl borate; MPEP, 2-methyl-6-(2-phenylethynyl)pyridine hydrochloride.

https://doi.org/10.1016/j.neuroscience.2018.06.016
0306-4522/

system, several Authors described the presence of mGluRs in the hair cell membrane of the frog labyrinth (Prigioni and Russo, 1995; Guth et al., 1998a,b; Hendricson and Guth, 2002a,b). In both inner ear organs, the role of such receptors would be to exert a feedback control on glutamate release. In the frog semicircular canal, hair cells have been shown to express mGluRs-I; the mGluR-I agonist, ACPD, produces an increase in the afferent firing rate, while the mGluR-I antagonists, 4-CPG and AIDA, prevent the ACPD-induced facilitation; these mGluR antagonists do not affect the resting firing rate (Guth et al., 1998b). mGluRs-I, which are coupled to G_q and phospholipase C (PLC), exert a positive feedback on transmitter release and shape the afferent information through calcium release from intracellular stores (Hendricson and Guth, 2002a). In recent years, the presence of a mechanism of calcium release from intracellular stores, via ryanodine receptors, was confirmed in the frog labyrinth: caffeine strongly increases the frequency of both spontaneous and mechanically evoked mEPSPs and spikes, while ryanodine decreases it. Neither drug affects mEPSP amplitude or time course (Lelli et al., 2003). Rossi et al. (2006) demonstrated that the selective mGluR-I agonist DHPG also increased mEPSP and spike frequency at the cytoneural junction, with no effects on mEPSP shape or amplitude; similar effects were produced by 2APB, a blocker of the sarcoplasmic-endoplasmic reticulum Ca-ATPase that increases cytosolic free calcium concentration. Receptors that activate the phospholipase C (PLC)-IP_3 pathway are therefore bound to raise intracellular calcium levels and enhance transmitter release.

Hendricson and Guth (2002b) observed that MPEP hydrochloride, another selective mGluR-I antagonist, also reduced the evoked discharge, without affecting the resting rate; the Authors concluded that the lack of effect on the resting discharge might contribute to further amplify the mechanically evoked transmitter release, enhancing signal discrimination in the afferent fibers.

Recently, increasing interest has been directed to mGluRs-II/III, which are expressed in the CNS as inhibitory autoreceptors and may be important in protecting neurons from excitotoxicity by predominantly activating $G_{i/0}$ proteins, which transduce by inhibiting adenylyl XI cyclase and by regulating ion channels via direct interaction of their $\alpha_{i/0}$ or $\beta\gamma$ subunits (Niswender and Conn, 2010 for a review). As of now, no data are available about the possible presence of mGluRs-II/III in labyrinthine organs, and in particular on hair cells.

Since it appears that several targets exist for glutamate at the cytoneural junction, this work was designed to explore and quantify the possible pre- and post-junctional effects of exogenous glutamate, to dissect the respective roles of AMPA and NMDA receptors at the postsynaptic membrane, to look for the presence of a glutamate transporter, and to test for the possible involvement of mGluRs-II/III in the presynaptic control of glutamate release. To this purpose, resting and mechanically evoked afferent discharges have been recorded in the isolated and intact frog labyrinth. In all experimental conditions the sensory discharge was analyzed in terms of spike rate and mEPSP amplitude, waveform and frequency, after detection and subtraction of spikes (Rossi et al., 2010, 2017; Martini et al., 2015). Patch-clamp experiments on the isolated hair cells have been performed to explore possible effects of glutamate on the calcium and potassium currents of the hair cells.

EXPERIMENTAL PROCEDURES

Our procedures followed the Principles of Laboratory Animal Care (86/609/EEC Directive of 1986), and were approved by the Italian Ministry of Health as well as by the Animal Care and Use Committee of the University of Ferrara. The experiments were performed at room temperature (20–22 °C) on frogs (*Rana esculenta*, 25–30 g body weight) purchased from authorized dealers. Animals were of the same geographical origin (Albania), and the experiments were preferably carried out in spring to minimize seasonally related variability. About one hundred frogs have been utilized in our experiments.

The frogs were anesthetized in tricaine methane sulfonate solution (1 g/l in tap water) and subsequently decapitated.

Intracellular recordings in the intact labyrinth

The posterior canal was exposed with its nerve in the right half of the frog head, bathed in a dissection solution of the following composition (mM): 120 NaCl, 2.5 KCl, 2 $CaCl_2$, 1 $MgCl_2$, 5 glucose, 5 Tris buffer (pH 7.3); 245 mOsmol/kg. The intact labyrinth was excised and fixed to the bottom of a small Perspex chamber (5 ml volume), mounted at the center of a small turntable, so that the posterior canal lay in the plane of table rotation. Mechanical stimulation was produced by subjecting the canal to sinusoidal angular velocity stimuli. Intracellular recordings were obtained at rest and during rotation using glass microelectrodes (30–40 MΩ resistance), filled with 3 M KCl, inserted into the posterior nerve within about 500 μm from the synapse. The recorded potentials were transferred through low-noise sliding contacts to the oscilloscope, recorded on tape, and analyzed off-line. The afferent discharge recorded from single fibers of the posterior nerve was evaluated in terms of spike frequency and of frequency and waveform of miniature excitatory postsynaptic potentials (mEPSPs).

Details of the experimental procedures have been described in previous papers (Martini et al., 2015; Rossi et al., 1994, 2006, 2010, 2017).

For each treatment to be tested, the preparation was recorded for 10 s at rest and then subjected to sinusoidal rotation at 0.1 Hz, 12.5 deg·s^{-2} maximal acceleration, on the plane of the posterior canal, for 50 s. The liquid in the chamber was then removed, the test solution was gently infused with a syringe, and the whole protocol (rest + stimulation) was repeated 4–5 times at 2-min intervals, while maintaining the recording from the selected fiber (“unit”). The following drugs have been tested: sodium glutamate (L-Glutamic acid monosodium salt monohydrate), CNQX (6-cyano-7-nitro quinoxaline-2,3-dione disodium salt hydrate), D-AP5

(D(−)-2-amino-5-phosphonovaleric acid), glycine, $MgCl_2$, LY341495 ((2*S*)-2-amino-2-[(1*S*,2*S*)-2-carboxycycloprop-1-yl]-3-(xanth-9-yl)propanoic acid), LY379268 ((1*R*,4*R*,5*S*,6*R*)-4-amino-2-oxabicyclo[3.1.0]hexane-4,6-dicarboxylic acid), DL-TBOA (DL-threo-β-benzyloxyaspartic acid). The source of LY341495, LY379268 and DL-TBOA was Tocris-Cookson (Bristol, UK). The source of sodium glutamate, CNQX, glycine, D-AP5, and of all other chemicals used in these experiments was Sigma (St. Louis, MO, USA).

LY341495, DL-TBOA, CNQX were dissolved in dimethyl sulfoxide. All the other chemicals were dissolved in water. Stock solutions were prepared for each drug and further diluted to the desired final concentrations in standard medium shortly before use.

Patch-clamp experiments

The procedures to dissect the two labyrinths and isolate the hair cells, as well as the recording techniques, have been reported in previous papers (Martini et al., 2000, 2007, 2009, 2013, 2015; Rossi et al., 2017). Potassium currents were recorded in a solution containing (mM): 120 NaCl, 2.5 KCl, 4 $CaCl_2$, 1 $MgCl_2$, 5 glucose, (Tris buffer, pH 7.3–7.5); the patch pipette was filled with (mM): 110 KCl, 2 $MgCl_2$, 8 ATP (K salt), 0.1 GTP (Na salt), 5 EGTA–NaOH, 10 HEPES–NaOH (pH 7.2; 235 mOsmol/kg). Calcium currents (ICas) were recorded in a solution containing (mM): 100 NaCl, 6 CsCl, 20 TEACl, 4 $CaCl_2$, 10 HEPES, 6 Glucose, pH = 7.2, 252 mOsmol/kg; the pipette solution composition was (mM): 90 CsCl, 20 TEA-Cl, 2 $MgCl_2$, 8–10 K-ATP, 0.1 Na-GTP, 10 HEPES, 5 EGTA (pH 7.2; 235 mOsml/kg).

In a first set of experiments, glutamate was applied to hair cells, holding the membrane potential at −100, −70 or −40 mV. In a second set of experiments, glutamate was tested on the ICa recorded in isolation. In a third set of experiments, glutamate or LY341495 were tested on the isolated delayed K currents, IKD. Each drug was applied by rapidly changing (typically < 50 ms) the external solution through the computer-controlled horizontal shift of a multibarreled perfusion pipette positioned in front of the recorded cell.

Quantal analysis

Electrophysiological recordings were analyzed according to a procedure that proved capable to measure mEPSP rates of occurrence above 100/s (Rossi et al., 2010, 2017). In this preparation, the general form of the elementary events (mEPSPs) is well represented by an analytical gamma distribution function of time: $w(t) = h \cdot (\beta t)^{\gamma} \cdot -\exp(-\beta t)/\Gamma(\gamma+1)$, where h (mV) is an amplitude factor, β (s^{-1}) is a rate constant, γ is a numeric coefficient that defines the shape of the waveform, and Γ indicates Euler's gamma function. Spikes were located, counted and digitally removed from the recording; a Wiener filter was built from the autoregressive fit on the autocorrelation of the spike-free recording and used to transform the tracing into a sequence of spiky events, which were automatically counted; the time of occurrence and waveform of each event were fit through a recursive least-squares optimization routine, applied to successive sections of the recording; detected events with peak amplitude < 0.1 mV were dropped; when the rank of the matrix of the waveforms of all fitted events was smaller than the number the events, those events that contributed most to the least-amplitude eigenvalue (s) of the covariance matrix were also dropped; conversely, new events were added when the fit fell short of the recorded signal; residual low-frequency fluctuations (< 10 Hz) in the baseline were compensated for.

The rate of occurrence of mEPSPs as a function of time was determined from the sequence of time intervals between successive events. Event rates up to 800/s could be reliably measured, even in the presence of high variability in individual event amplitude and waveform.

The subtraction of spikes unavoidably canceled some mEPSPs; based on previous analyses (Rossi et al., 2010), mEPSP counts were corrected by adding five events in the 3-ms interval corresponding to each subtracted spike.

The overall time courses of mEPSP and spike rates of occurrence were displayed and the total number of events were counted during 10 s of the resting phase, during the excitatory (5 s) and the inhibitory (5 s) hemicycles in the first rotation, as well as during three rotation cycles (30 s). The size distribution of mEPSP was also obtained during each period. The average event waveform was obtained by manually selecting several events (detected through a multistage thresholding procedure) that were free of overlaps for most of their time course. The above-mentioned analytical function, $w(t)$, was fitted to the average mEPSP waveform, in control and experimental conditions, by minimizing the square errors (Rossi et al., 1994).

Data analysis

All data are reported as mean ± SEM. Comparisons were always made between different conditions in the same unit and were evaluated through Student's paired *t*-test whenever a normal distribution could be assumed or verified; otherwise, the Wilcoxon signed-rank test was applied; in this case, the value of Wilcoxon's statistic W is reported (degrees of freedom in parentheses) together with the pseudo-median difference (absolute, Δ, or percentage, %Δ), the rank correlation (ρ^2) and *P* value. Values of $P \leq 0.05$ were considered significant.

All routines for quantal analysis were developed in Matlab software environment (Version 10a, The MathWorks, Natick, MA, USA). The figures were prepared using a commercial plotting program (Sigmaplot, Version 11.0, Jandel Scientific, San Rafael, CA, USA).

RESULTS

Glutamate on the afferent discharge

Endogenous glutamate is released at high rate at the posterior canal cytoneural junction to sustain the high-frequency discharge observed at rest and during

mechanical stimulation; no synaptic fatigue appears to ensue during long-lasting and repetitive stimulation (Martini et al., 2015).

Bath application of glutamate (5 mM) produced a clear increase in mEPSP and spike frequencies. An example is illustrated in Fig. 1, which displays the sensory discharge at rest and during sinusoidal rotation at 0.1 Hz (peak acceleration 12.5 deg·s^{-2}) in one unit in control (A) and during the application of 5 mM sodium glutamate (B). The smoothed time courses (1-s time constant) of the sensory discharge frequency (mEPSPs/s and spikes/s) are also shown (panels (E) and (F)): notice that both in control and in the presence of glutamate the mechanical stimulation produces an overall enhancement of release, so that the minimum frequencies during the inhibitory hemicycle are comparable to the frequencies recorded at rest (during the first 10 s of each trace).

Eleven units were examined before and after the application 5 mM glutamate. The presynaptic effect of glutamate on the sensory discharge developed soon, reached a maximum after 2–3 min, persisted for at least 7–8 min more, and then vanished. The sensory discharge generally returned to control value; earlier desensitization ensued in a few fibers only. The application of glutamate did not prevent the normal excitatory and inhibitory modulation of the discharge by mechanical stimuli; nor did it produce any depolarization of the postsynaptic fiber.

Three of these units did not display any spike activity in control solution.

Results are graphically displayed in Fig. 2 and summarized in Tables 1 and 2.

Exogenous glutamate did not significantly affect the amplitude of the unitary event: the peak value of the single mEPSP averaged 0.55 ± 0.12 mV in the presence of glutamate (10,308 events) vs 0.39 ± 0.04 mV in control (8,912 events); the comparison did not indicate any significant difference ($P > 0.1$, paired t-test, $n = 11$). In order to verify that the mEPSP identification procedure worked correctly, a peak amplitude distribution was computed and examined for each experiment, to make sure that such distribution was lognormal and unimodal, thereby excluding the presence of a significant number of ‘‘double-sized” events, which would result if our procedure were not able to split almost coincident events at high occurrence

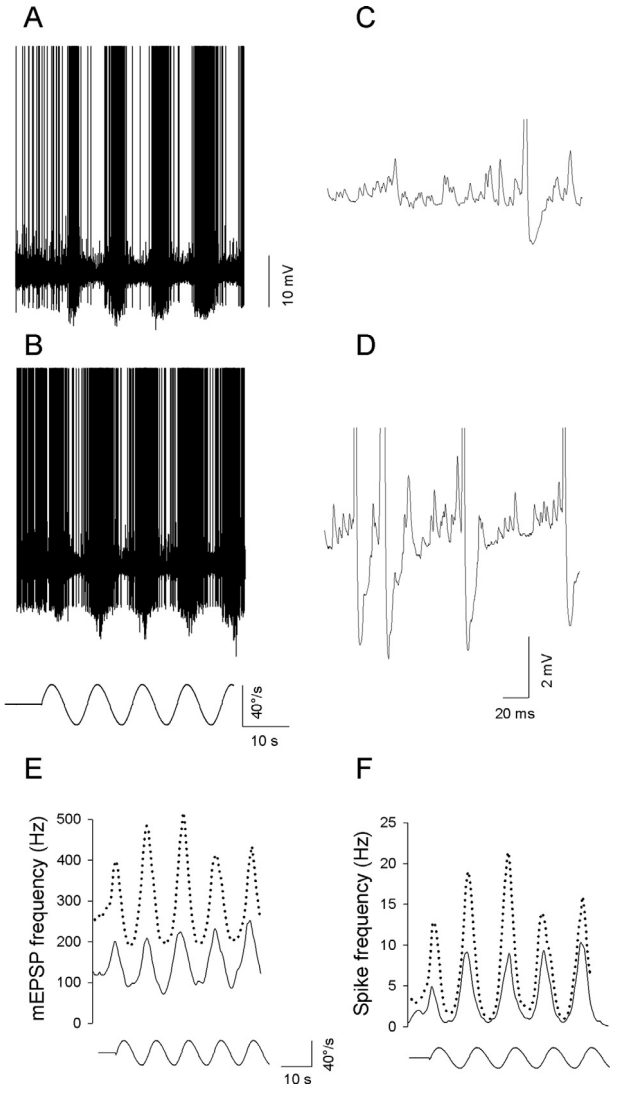

Fig. 1. The effect of 5 mM sodium glutamate on the resting and evoked sensory discharge in a posterior canal unit. Panels (A) and (B) illustrate mEPSP and spike discharge at rest (first ten seconds) and during mechanical sinusoidal rotation (0.1 Hz, peak acceleration 12.5 deg·s^{-2}), in control Ringer solution and in the presence of 5 mM sodium glutamate, respectively. Turntable angular velocity during rotation is illustrated below. Small sections of the resting discharge in control solution and after glutamate application are displayed on a finer time scale in (C) and (D), respectively. Action potentials are truncated in A–D. Panels (E) and (F) show the smoothed time course (1-s time constant) of mEPSP and spike frequency, at rest and during rotation, in the same posterior canal unit, in control (continuous lines) and in the presence of 5 mM sodium glutamate (dotted lines), respectively. Turntable angular velocity is illustrated at the bottom.

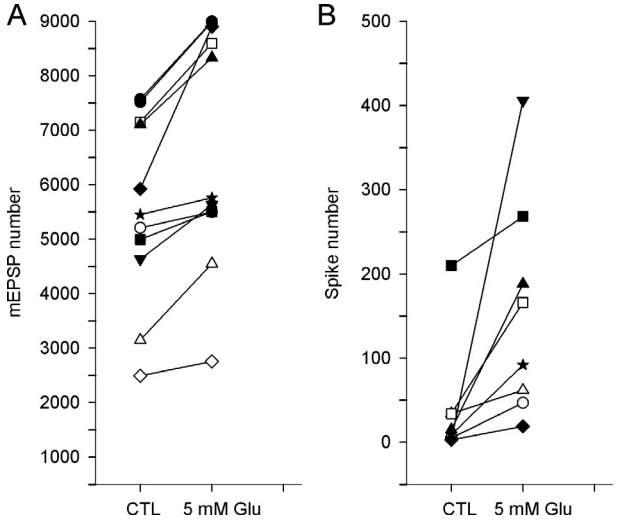

Fig. 2. The enhancement of mESP and spike rates by 5 mM glutamate. Panels (A) and (B) respectively illustrate the number of mEPSPs or of spikes discharged during three cycles of rotational stimulation at 0.1 Hz (peak acceleration 12.5 deg·s^{-2}) by 11 distinct units in control solution or 2 min after applying 5 mM Glu. Three of these units did not display spike activity.

Table 1. Maximal effects of 5 mM glutamate on mEPSP discharge properties at rest or during sinusoidal stimulation (0.1 Hz, 12.5 deg·s^{-2}). Mean ± SEM; n = 11. Wilcoxon's signed rank test

	Control	5 mGlu	%Δ	Stats
Spontaneous activity (mEPSPs/s)	166 ± 19	213 ± 16	+26	**
Number of mEPSPs in the exc. hemicycle	1064 ± 91	1341 ± 98	+22.5	**
Number of mEPSPs in the inhib. hemicycle	800 ± 88	1012 ± 104	+22	**
Number of mEPSP in the first cycle	1880 ± 179	2336 ± 197	+25.4	**
Number of mEPSPs in three cycles	698 ± 581	6491 ± 604	+12.7	*

%Δ: difference pseudomedian (% of control median).
** $W(11) = 66$; $\rho^2 = 1.0$, $P \leq 0.001$.
* $W(11) = 46$; $\rho^2 = 0.83$, $P \leq 0.05$.

Table 2. Maximal effects of 5 mM glutamate on spike discharge properties at rest or during sinusoidal stimulation (0.1 Hz, 12.5 deg·s^{-2}). Mean ± SEM; n = (8). Wilcoxon's signed rank test

	Control	5 mM Glu	Δ	stats
Spontaneous activity (Spikes/s)	0.8 ± 0.4	8.4 ± 1.9	6.29	*
Number of Spikes in the exc. hemicycle	11.2 ± 7.5	36.3 ± 9.2	19.5	*
Number of Spikes in the inhib. hemicycle	2.6 ± 0.9	18.3 ± 3.3	14	*
Number of Spikes in the first cycle	13.7 ± 8.2	51.1 ± 12.5	24	*
Number of Spikes in three cycles	39.1 ± 24.8	156.0 ± 46.2	70.5	*

Δ: difference pseudomedian.
* $W(8) = 36$; $\rho^2 = 1.0$, $P \leq 0.01$.

rates. Examples of such distributions are displayed in Fig. 3. In all situations the amplitude distribution during spontaneous activity was compared with that during the excitatory hemicycle of mechanical stimulation, where rates generally were much higher: the two distributions were quite precisely superimposable, thereby reassuring us that the procedure behaved well at high frequencies as well. The average values remained unaltered, which demonstrates that changes in event frequency or amplitude are well distinguished by the procedure. The shapes of the distributions were almost identical: they remained unimodal and did not show any detectable changes toward the high amplitude values, where possible unresolved multiple events would fall. This analysis confirmed that glutamate did not modify the amplitude distribution of the events (Fig. 3A, B), although their frequency was much enhanced; this also confirms that no significant inactivation of the receptor occurs in the presence of 5 mM glutamate.

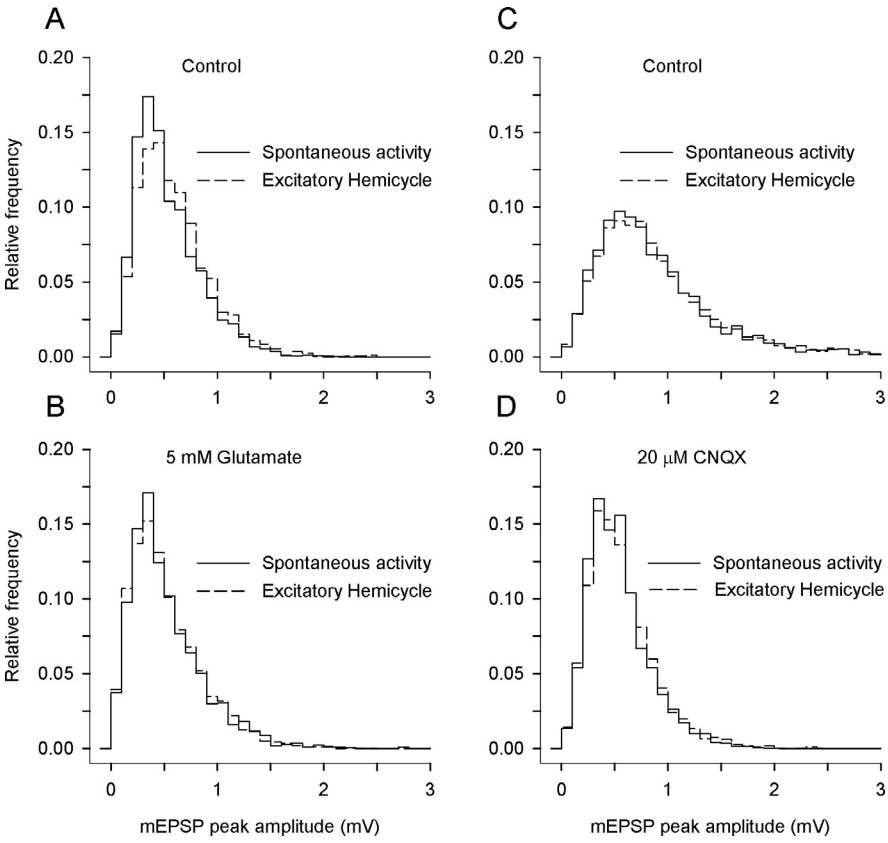

Fig. 3. The amplitude distribution of mEPSPs under various conditions. Panels (A) and (B) compare the amplitude distribution of mEPSPs in the same unit in control and 2 min after applying 5 mM glutamate. In both panels the distributions observed at rest (continuous lines, 794 events in control, 817 in glutamate) or during the excitatory hemi-cycle (dashed lines, 861 events in control, 1,156 in glutamate) are superimposed to show that the increase in mEPSP frequency does not affect their amplitudes. The distributions observed in glutamate are quite similar to those in control conditions. Panels (C) and (D) compare the amplitude distribution of mEPSPs in the same unit in control (781 events at rest, 1093 during the excitatory hemicycle) and in the presence of 20 μM CNQX (1022 events at rest, 1049 during the excitatory hemicycle). The distributions in CNQX are clearly contracted toward lower values, consistent with a decrease in the average amplitude of the mEPSPs.

Effects of ionotropic glutamate receptor blockers (postsynaptic effects)

To test the sensitivity of postsynaptic AMPA receptors, increasing

concentrations of CNQX (1, 10, 20, 50 μM) were applied. Each concentration was tested on a group of 5 fibers. For every fiber, mEPSP peak size was evaluated in control and in the presence of the drug on a large number of events recorded at rest (10 s), and during the first excitatory (5 s) and inhibitory hemicycles (5 s).

CNQX proved able to significantly decrease mEPSP amplitudes. An example of the effect of 20 μM CNQX on the probability distribution of mEPSP amplitudes is displayed in Fig. 3C and D. Notice that in this case as well the histograms obtained at rest or during the excitatory half-cycle are virtually superimposable.

The dose–response relation of CNQX effect on the mean mEPSP peak amplitude is illustrated in panel (A) of Fig. 4. The mEPSP size in the presence of the different CNQX concentrations was normalized in each unit to the corresponding mean value in control solution.

Data were fitted by a standard four-parameter logistic curve: $S(C_I) = S_\infty + \frac{S_0 - S_\infty}{1+(C_I/K_I)^H}$, where $S(C_I)$ is mEPSP average size, C_I is the concentration of the inhibitor (CNQX), K_I is its affinity, S_0 and S_∞ represent mEPSP size in the absence and in the presence of maximal concentration of the antagonist, and H is Hill slope coefficient. The estimates of K_I were quite consistent at rest (21.6 μM) and during stimulation: 20.7 and 18.1 μM for the excitatory and inhibitory hemicycles, respectively. The goodness of fit correlation coefficient (R^2) was > 0.98 in all three conditions. The estimates of Hill coefficient under the same conditions were quite close to unity (0.96, 1.05 and 1.17); so the fits were repeated after fixing Hill coefficient to unity; the corresponding estimates of K_I became 20.6 μM at rest and 22.6 μM during both the excitatory and inhibitory phases of mechanical stimulation. R^2 values remained > 0.98.

The mEPSP average peak sizes and frequencies in control and in the presence of increasing concentrations of CNQX are reported in Table 3.

To evaluate possible changes in mEPSP parameters due to CNQX effect, the waveforms of isolated events were examined: events were detected through a multistage thresholding procedure and those that were free of overlaps for most of their time course were selected and aligned on their occurrence time. The average time course was fitted, in control and experimental conditions, by setting the parameters of the above-mentioned analytical function, $w(t)$, to the values (± SEM) that minimized the square errors (Rossi et al., 1994). An example is shown in panels B (control) and C (CNQX) of Fig. 4. The corresponding parameters of the gamma-distribution functions were: shape factor γ = 1.98 ± 0.07, rate constant β = 1.93 ± 0.06 kHz, time-to-peak = 1.02 ± 0.008 ms in the presence of 10 μM CNQX (n = 90) vs. γ = 2.17 ± 0.06, β = 1.76 ± 0.04 kHz, time-to-peak = 1.23 ± 0.01 ms in control (n = 118). The only parameter deeply affected by the drug was the peak value (1.35 ± 0.04 mV under CNQX treatment vs 1.73 ± 0.04 in control; −28%; paired t-test, $t(4) = -6.81$, $P \leq 0.005$). When the time-to-peak was considered in four units, it turned out to be slightly but not significantly faster in CNQX than in control solution (−12.6%, $t(3) = -2.09$, P value n.s.) due to a corresponding increase in the decay rate constant β (+30%, $t(3) = -2.131$, P value n.s). This analysis could only be applied to selected units that displayed a relatively low mEPSP frequency (< 100/s, n = 5).

Although the literature suggests that NMDA receptors are not present in our preparation, it seemed important to check for their possible presence, by testing the effects of the NMDA-R blocker D-AP5 at various concentrations (10, 20, 50, 100, 200 μM). The mean mEPSP amplitude remained fairly constant upon raising D-AP5 concentration up to 100 μM. Only the 200 μM concentration did produce a significant decrease in the mean mEPSP peak size. This may well be ascribed to unspecific binding to AMPA receptors. The

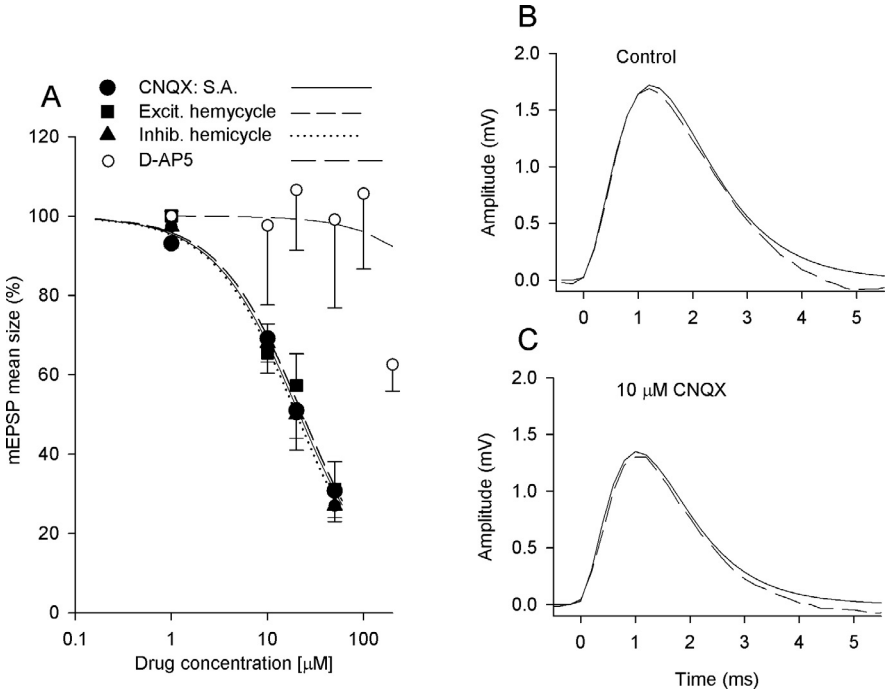

Fig. 4. The effect of ionotropic glutamate receptor antagonists on mEPSP size and waveform. The effect of various concentrations of CNQX is depicted in pane A. Five units were tested for each CNQX concentration. The dose–response curve was evaluated during the spontaneous activity (filled circles), the excitatory (squares) and inhibitory (triangles) hemicycles. The resulting K_I values are nearly identical (range 20–23 μM). The effect of D-AP5, on a total of 26 units, is also illustrated (empty circles) for comparison: a decrease in mEPSP size was only observed at 200 μM. Error bars depict SEMs. Panels (B) and (C) display the analytical fits to mEPSP waveforms in control and under the effect of 10 μM CNQX (4 min), respectively. For either condition the averaged time course of elementary events (dashed line) and the corresponding fit (continuous line) with gamma-distribution functions are displayed (118 mEPSPs in (B) and 90 in (C)). The peak amplitude of the averaged events and the fit parameters are reported in the text.

Table 3. mEPSP peak size and frequency (s^{-1}) in control and in the presence of increasing concentrations of CNQX. Mean ± SEM; $n = 5$ (for each unit the number of events ranged from 3000 to 13,200). Student's *t*-test

[CNQX] (μM)	mEPSP peak size (mV)				mEPSPs/s	
	Control	CNQX	Diff. (%)	*P*	Control	CNQX
1	0.62 ± 0.09	0.62 ± 0.009	0	(n.a.)	215	218
10	1.06 ± 0.11	0.76 ± 0.09	−28 ± 4	≤0.005	221	241
20	1.06 ± 0.28	0.51 ± 0.11	−52 ± 4	≤0.001	123	101
50	0.85 ± 0.18	0.24 ± 0.03	−72 ± 2	≤0.02	232	222

resulting dose–effect curve is shown in panel A of Fig. 4, superimposed onto that for CNQX. The mEPSP peak size in control and in the presence of different concentrations of D-AP5, as well as the corresponding mEPSP frequencies, are reported in Table 4.

NMDA-Rs require depolarization-induced removal of Mg from the pore and the binding of glycine as a cofactor. We therefore performed experiments in which mEPSP peak size and frequency were compared in control Ringer solution (containing 1 mM Mg) and in Mg-free Ringer solution containing 2 mM Ca^{2+}. Various concentrations of D-AP5 (10–20–50–100–200 μM) and glycine (10–50 μM) were employed. Results are summarized in Table 5 and confirm that the drug has no specific effect.

Drugs acting on mGluRs (presynaptic effects)

The mGluRs-II/III agonist, LY379268, did not display any effect on the parameters of mEPSP discharge (concentration range: 10–100 μM). Prolonged pre-treatment with various drug concentrations, applied to the bath for at least half an hour, did not produce any evident change with respect to control recordings.

Conversely, the antagonist LY341495 produced a consistent increase in mEPSP and spike numbers. This presynaptic effect was concentration dependent in the 0.01–50 μM range. The increase in mEPSP and spike numbers was already significant (Wilcoxon's signed rank test) at 10 nM, during the first stimulation cycle, both for mEPSPs ($W(6) = 21$, $\%\Delta = 16.6\%$, $\rho^2 = 1$, $P \leq 0.05$) and for spikes ($W(6) = 21$, $\%\Delta = 350\%$, $\Delta = 7$/s, $\rho^2 = 1$, $P \leq 0.05$,) as well as during the whole 30-s stimulation period ($W(6) = 21$, $\%\Delta = 10.4\%$, $\rho^2 = 1$, $P \leq 0.05$ for mEPSPs and $W(6) = 21$, $\%\Delta = 176.3\%$, $\Delta = 15.5$/s, $\rho^2 = 1$, $P \leq 0.05$ for spikes). In all the fibers tested during rotation with the different LY341495 concentrations, significant increases in mEPSP and spike numbers (up to 163% and to 1284%, respectively), were observed during the first stimulation cycle (Wilcoxon's signed rank test: $W(6) = 21$, $\Delta\% = 154\%$, $\rho^2 = 1$, $P \leq 0.05$ for mEPSPs; $W(6) = 21$, $\%\Delta = 1183$, $\Delta = 86$/s, $\rho^2 = 1$, $P \leq 0.05$ for spikes). Similarly, mEPSP and spike numbers significantly increased (up to 138% and to 2613%, respectively) during the three stimulation cycles ($W(6) = 21$, $\%\Delta = 150.6\%$, $\rho^2 = 1$, $P \leq 0.05$ for mEPSPs; $W(6) = 21$, $\%\Delta = 1705\%$, $\Delta = 251.5$/s, $\rho^2 = 1$, $P \leq 0.05$ for spikes).

Table 4. Effects of D-AP5 on mEPSP peak size (mV) and frequency (s^{-1}). In each unit mEPSP size and frequency were evaluated at rest and during stimulation. Mean ± SEM. Student's *t*-test

D-AP5 (μM)	mEPSP peak size (mV)				mEPSPs/s	
	Control	D-AP5	Diff. (%)	*P*	Control	D-AP5
10 ($n = 3$)	1.12 ± 0.21	1.10 ± 0.22	−2.7 ± 2.9	n.s.	329 ± 47	336 ± 47
20 ($n = 5$)	0.95 ± 0.12	1.01 ± 0.14	8.1 ± 10.8	n.s.	306 ± 42	316 ± 43
50 ($n = 6$)	0.92 ± 0.19	0.91 ± 0.18	0.2 ± 3.0	n.s.	281 ± 31	278 ± 26
100 ($n = 6$)	0.81 ± 0.13	0.86 ± 0.15	7.4 ± 8.6	n.s.	251 ± 43	259 ± 35
200 ($n = 6$)	1.00 ± 0.11	0.62 ± 0.06	−36.9 ± 1.6	≤0.001	224 ± 24	207 ± 18

Table 5. Lack of effect of Mg-free solutions, either in absence or in presence of various concentrations of glycine and D-AP5. The average mEPSP peak size and frequency were evaluated at rest and during stimulation (Mean ± SEM). No comparison gave a significant change

D-AP5 (μM)	Glycine (μM)	n.	mEPSP peak size (mV)			mEPSP/s	
			Control	0 Mg	Diff % (n.s.)	Control	0 Mg
0	0	4	1.02 ± 0.23	0.97 ± 0.20	-2.2 ± 5.9	237 ± 41.2	234 ± 36.1
0	10	2	0.80 ± 0.14	0.73 ± 0.09	-8.0 ± 4.9	347 ± 84.0	327 ± 67.0
0	50	4	1.10 ± 0.08	1.09 ± 0.11	-0.6 ± 4.4	216 ± 14.5	194 ± 14.6
50	50	4	0.63 ± 0.06	0.64 ± 0.05	1.6 ± 4.0	241 ± 27.0	243 ± 21.5
100	50	4	0.83 ± 0.17	0.91 ± 0.19	12.5 ± 9.0	215 ± 30.7	235 ± 33.7

Fig. 5 shows the net increase in mEPSP and spike numbers produced by increasing LY341495 concentrations.

In all the fibers tested during rotation with the different LY341495 concentrations, a significant increase in mEPSP ($W(6) = 21$, $\%\Delta = 118.4\%$, $\rho^2 = 1$) and spike frequency ($W(6) = 21$, $\%\Delta = 558\%$, $\Delta = 12$/s, $\rho^2 = 1$) was observed also at rest (all P values ≤ 0.05).

In some units, 5 mM glutamate was added in the presence of various concentrations of LY341495 (0.01, 0.50, 1 μM); this produced a further increase in resting and mechanically evoked mEPSP and spike frequency, as illustrated for a unit in Fig. 6, suggesting a cooperative effect of mGluR-I activation by glutamate and mGluR-II/III inhibition by LY341495. The cumulative results from 6 units are graphically illustrated in Fig. 7.

Under this condition, during the 8 min of the full protocol (four repetitions of the resting + stimulus sequence) clear desensitization was observed. An example is illustrated in Fig. 8: the control recording, the facilitatory effect of 5 mM Glu and the late desensitization, 6 min after glutamate application, are shown in (A)–(C), respectively. The panels on the right hand side show portions of the same recordings on a more expanded time scale. The lower trace in panel (E) in particular shows how the recording is fit by splitting it into many elementary events (mEPSPs): even under this condition of particularly intense activation the routine is able to isolate mEPSPs of reasonably similar size; a few possible double (synchronous) events can be seen, but they are not in such a number to significantly affect the total mEPSP counts or their amplitude distribution. Panel F shows that during desensitization the size of the elementary events, rather than their frequency, declines at later times. Under this condition the resting and mechanically evoked sensory discharge finally waned by some 10 min. Desensitization disappeared upon returning to the control solution (not shown).

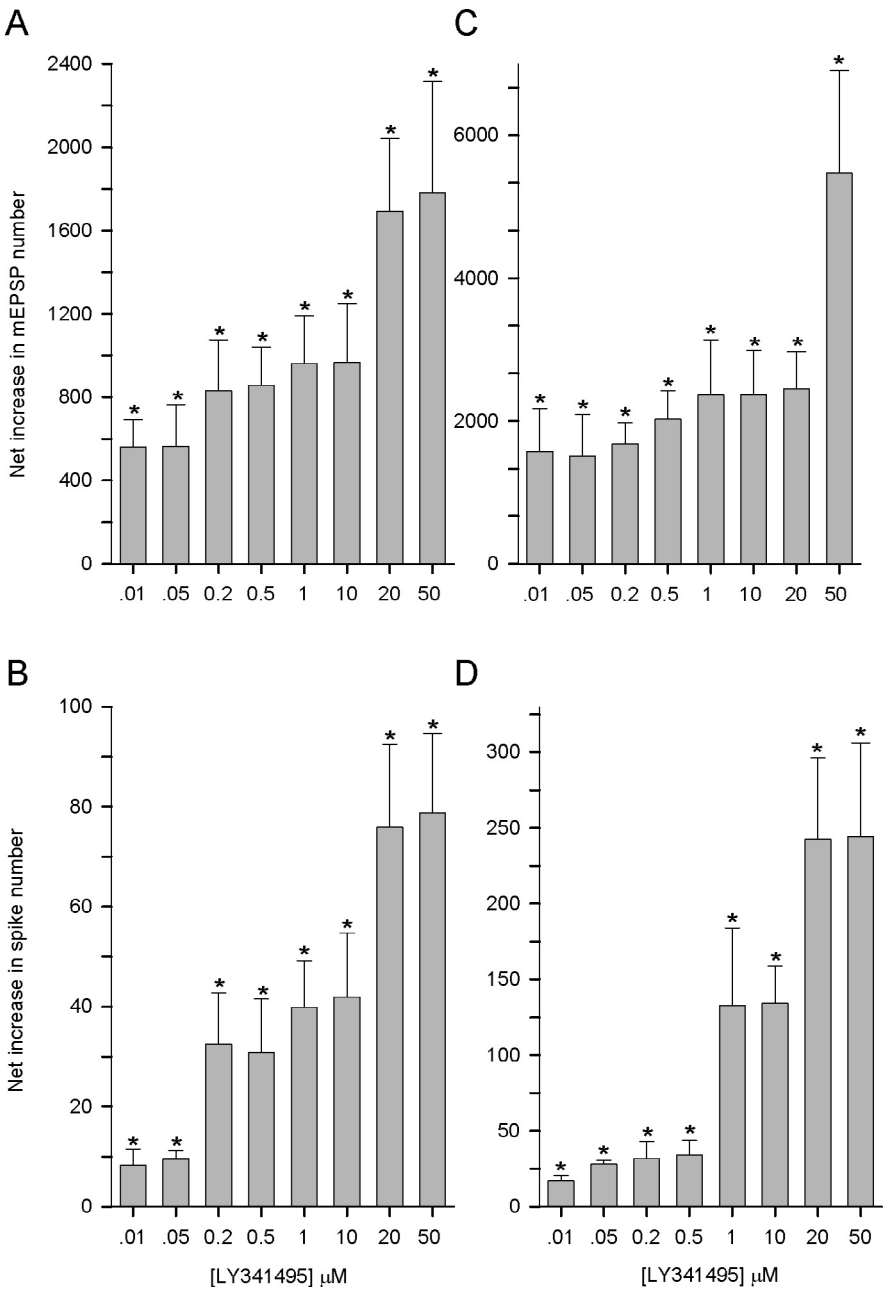

Fig. 5. The effect of increasing LY341495 concentrations (range: 0.01–50 μM) on the evoked afferent mEPSP and spike numbers. The bars (mean ± SEM) in panels (A) and (B) show the net increase in mEPSP and spike numbers, respectively, during the first stimulation cycle. The bars (mean ± SEM) in (C) and (D) illustrate the net increase in mEPSP and spike numbers, respectively, during three stimulation cycles (30 s). Stars indicate statistically significant differences from control (see text for statistical comparison).

Inhibition of glutamate transporter

DL-TBOA is a broad-spectrum glutamate transporter antagonist. It systematically produced an increase in mEPSP and spike number when applied to the semicircular canal at concentrations ranging 20–300 μM. Similar to bath application of glutamate, mEPSP peak amplitudes were unaffected (not shown).

The sensitivity of the afferent discharge to DL-TBOA was quite variable in the various units tested. The effect of DL-TBOA developed slowly and kept increasing for the first 6–8 min at least, during the repeated stimulation protocol described in the *Methods*. Given such a duration of the experiment, testing several different concentrations on the same unit was not possible; therefore the results

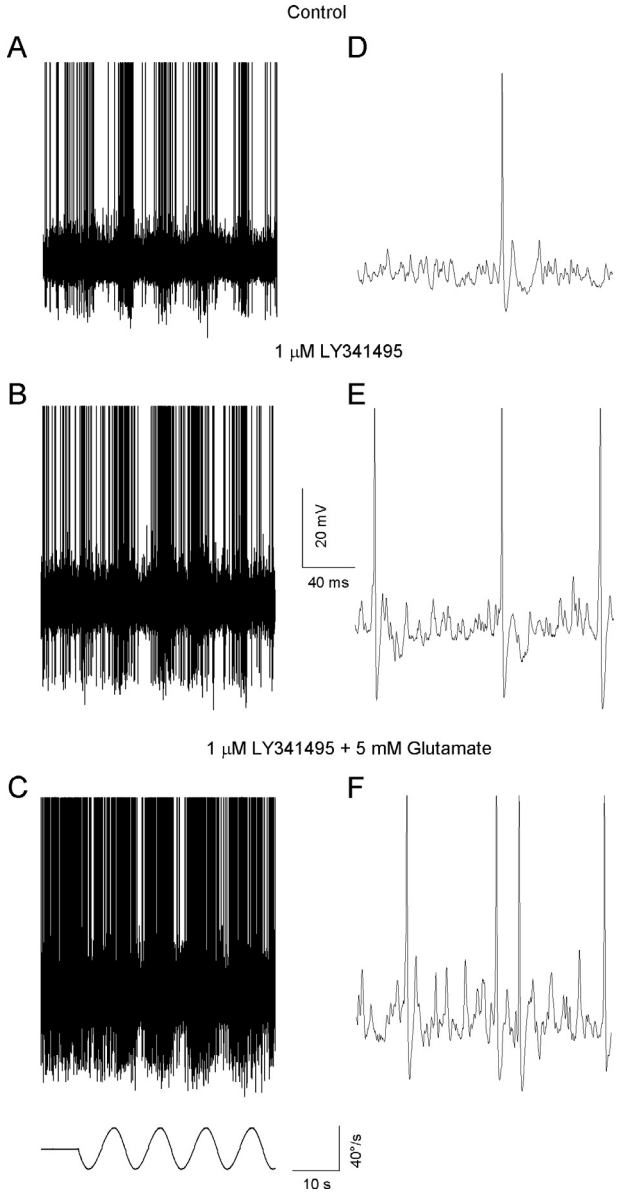

Fig. 6. An example of the cumulative effect of LY341495 and sodium glutamate on the sensory discharge of a posterior canal afferent unit. A illustrates the resting and mechanically evoked afferent discharge in control solution; B illustrates the effect of 1 μM LY341495 (after 3 min) on the same unit; C shows the cumulative effect of 1 μM LY341495 + 5 mM sodium glutamate (after 6 min) in the same unit. The panels (D)–(F) show portions of the recording in (A–C), respectively, taken during the resting discharge, on a faster time scale. Action potentials are truncated in all panels. Turntable angular velocity is illustrated at the bottom.

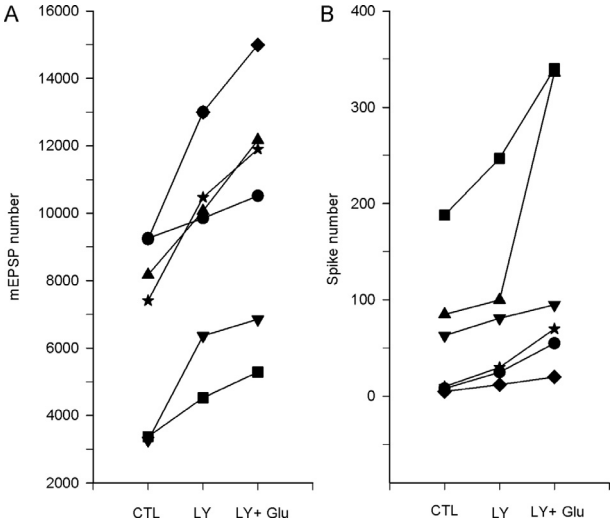

Fig. 7. The effect of LY341495 and sodium glutamate on mEPSP and spike rates. The graphs display the number of mEPSPs (Panel (A)) or of spikes (B) measured in six fibers during three cycles of mechanical rotational stimulation in control condition, 2 min after applying 1 μM LY341495 or 4 min after the cumulative addition 1 μM LY341495 + 5 mM sodium glutamate. The increases in both mEPSP and spike rates are quite variable, but they are systematically present.

obtained with 20, 50, 100 μM were pooled together (3 units for each concentration for EPSPs, while only 2 for each concentration could be used for spikes as 3 units tested did not display any spike activity). The increases in mEPSP and spike numbers were significant (Wilcoxon's signed rank test), during the first stimulation cycle ($W(9) = 45$, $\%\Delta = 31.7\%$, $\rho^2 = 1$, $P \leq 0.005$ for mEPSPs and $W(6) = 21$, $\%\Delta = 98.4\%$, $\Delta = 14$/s, $\rho^2 = 1$, $P \leq 0.05$ for spikes) as well as during the three stimulation cycles ($W(9) = 43$, $\%\Delta = 35.7\%$, $\rho^2 = 0.79$, $P \leq 0.001$ for mEPSPs and $W(6) = 21$, $\%\Delta = 184.5\%$, $\Delta = 25.5$/s, $\rho^2 = 1$, $P \leq 0.05$ for spikes). Similar increases in the parameters of discharge were observed with higher DL-TBOA concentrations (200–300 μM, $n = 3$ for 200 μM, and $n = 4$ for 300 μM): $W(7) = 28$, $\%\Delta = 31.7\%$, $\rho^2 = 1$ for mEPSPs and $W(7) = 28$, $\%\Delta = 100\%$, $\Delta = 18$/s, $\rho^2 = 1$, $P \leq 0.05$ for spikes during the first cycle, and $W(7) = 28$, $\%\Delta = 23.2\%$, $\rho^2 = 1$, $P \leq 0.05$ for mEPSPs and $W(7) = 28$, $\%\Delta = 76.4\%$, $\Delta = 56$/s, $\rho^2 = 1$, $P \leq 0.05$ for spikes, during the three cycles. The net increases in mEPSP and spike numbers produced DL-TBOA are illustrated in Fig. 9A, B for the first cycle and in Fig. 9C, D for the three cycles (30 s).

Similar to LY341495, DL-TBOA also affected the resting mEPSP and spike frequency of all fibers at all the tested concentrations (20, 50, 100 μM and 200, 300 μM): significant increases (Wilcoxon's signed rank test) were reported both for mEPSP frequencies ($W(9–7) = 45/28$, $\%\Delta = 29.7–63.1\%$, $\rho^2 = 1$, P values between ≤ 0.005 and ≤ 0.05) and for spike rates ($W(6–7) = 21–28$, $\%\Delta = 398–156.9\%$, $\Delta = 3.75–2.51$/s, $\rho^2 = 1$, all P values ≤ 0.05).

In some units, 5 mM glutamate was added in the presence of various concentrations of DL-TBOA (20, 50, 200 μM); this produced a further increase in resting and mechanically evoked mEPSP and spike frequency. In those units in which good recordings could be maintained for relatively long time, at rest and during repetitive mechanical stimulation (8–10 min), DL-TBOA plus 5 mM glutamate sometimes did produce desensitization of postsynaptic AMPA receptors. An example of the facilitatory effect of DL-TBOA (200 μM) on the afferent discharge in a unit is illustrated in Fig. 10, panels B, E; panels C, F in the same figure

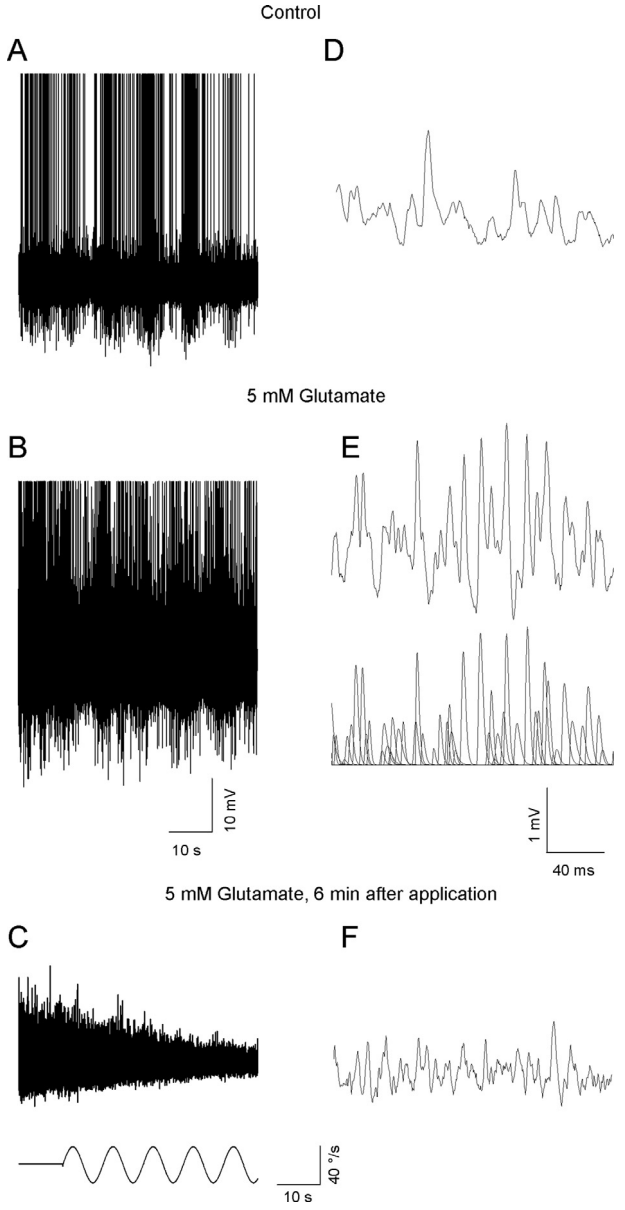

Fig. 8. The desensitization of the postsynaptic AMPA receptors. (A) Shows the resting and mechanically evoked sensory discharge in an afferent unit in control solution. (B) Illustrates the recording from the same unit in the presence of 5 mM Glutamate. (C) Shows a later recording, illustrating the desensitization of the AMPA receptors 6 min after Glutamate application. Desensitization disappeared on returning to the control solution (not shown). Panels (D)–(F) display small sections of the recordings taken in (A)–(C) on a faster time scale. The decomposition of the signal into elementary events (mEPSPs), produced by the analysis procedure, is also displayed in (E) (bottom trace): this indicates that the increased fluctuations in the recording are due to increased mEPSP rate and the resulting mEPSP summation, rather than to an increase in their size. In (F) the desensitization can be seen to affect the size of the events rather than their frequency. Action potentials are truncated in (A) and (B). The turntable angular velocity is displayed at the bottom.

show the cumulative effect of 200 μM DL-TBOA + 5 mM Glutamate. This additive effect is similar to what illustrated above for 1 μM LY341495 (see Fig. 6).

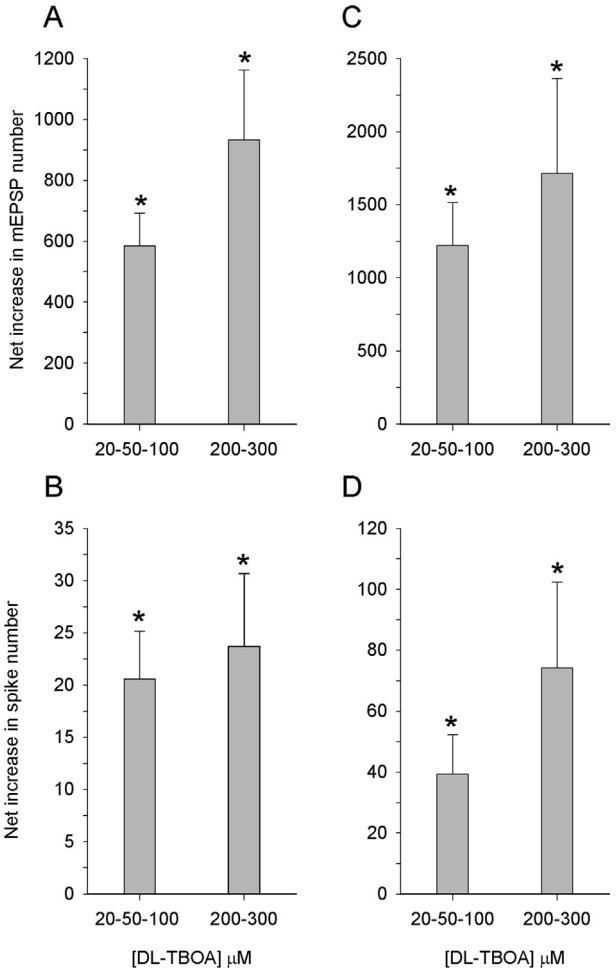

Fig. 9. The effect of various DL-TBOA concentrations (range: 20–300 μM) on the evoked afferent mEPSP and spike numbers. The bars (mean ± SEM) in panels (A) and (B) show the net increase in mEPSP and spike numbers, respectively, during the first stimulation cycle. The bars (mean ± SEM) in (C) and (D) illustrate the net increase in mEPSP and spike numbers, respectively, during three stimulation cycles (30 s). Stars indicate statistically significant differences from control (see text for statistical comparison). Three units were tested for each concentration in the range 20–50–100 μM (2 units for spikes, since 3 units did not display any spike activity). For higher concentrations, 3 units were tested with 200 μM, and 4 units with 300 μM.

The actions of glutamate on the hair cell

Since the drugs here used proved able to affect junctional discharge, pointing to the presence of prejunctional glutamate receptors, it seemed important to investigate whether glutamate itself was able to produce any detectable bioelectric effect on the hair cell.

Using the whole-cell patch-clamp recording technique, we explored whether the application of 2 mM glutamate produced any changes in cell conductance, holding the membrane potential at −70 mV. No consistent change was observed in holding current (−9.41 ± 1.58 in glutamate vs −8.60 ± 1.42 pA in control, $n = 3$; difference = −0.81 ± 0.37). Similarly, no evident changes were observed when glutamate was applied at −100 or −40 mV holding potentials (data not shown).

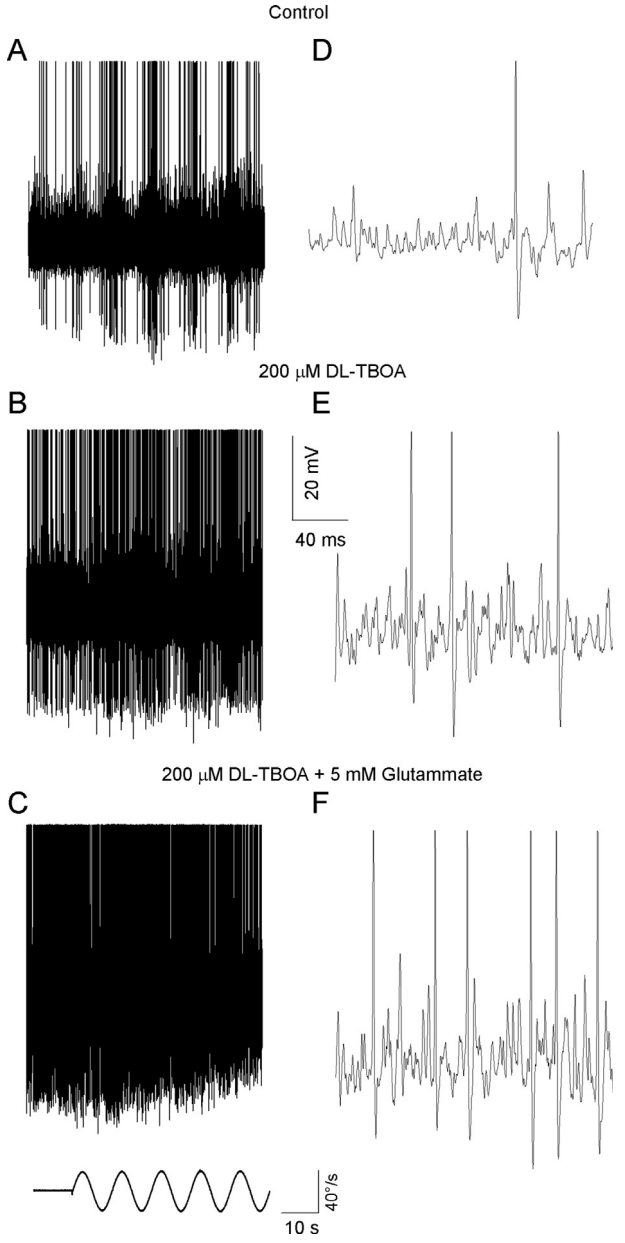

Fig. 10. Example of the effects of 200 μM DL-TBOA on junctional activity. The panels on the left-hand side depict the electrophysiological recordings obtained from an exemplar unit in control solution (A), after adding 200 μM DL-TBOA (B) and after the further addition of 5 mM glutamate (C). Turntable angular velocity is illustrated at the bottom. The panels on the right-hand side are short sections of the corresponding recordings on the left, on a finer time scale, that better illustrate the increasing rates of both mEPSPs and spikes. Spikes are truncated in all panels. A late sign of desensitization is apparent in panel (C), as the junctional noise gradually declines toward the end of the stimulation.

Possible effects on voltage-dependent conductances were examined by recording calcium and potassium currents. The biophysical properties of the hair cell ICa have been previously described (Martini et al., 2000, 2007). ICas were recorded from isolated hair cells in control solution and during the application of 2 mM glutamate (repetitive applications and recovery in control solution). No effects of 2 mM sodium glutamate were observed.

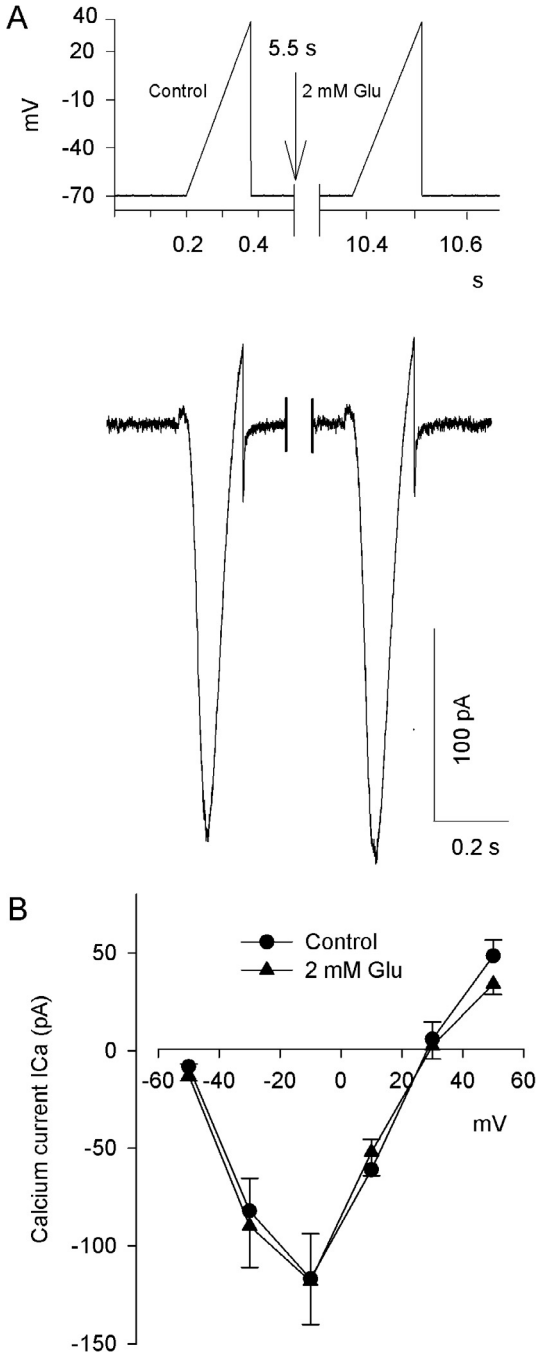

Fig. 11. Lack of effect of sodium glutamate on the calcium current recorded in isolated hair cells. The calcium current (ICa) amplitude during 180-ms voltage ramps from −70 to +40 mV is shown in panel (A) for an exemplar cell in control solution, on the left, and in the presence of 2 mM glutamate, on the right. The peak current value was −230 ± 75 in the presence glutamate versus −222 ± 73 pA in control. Panel (B) illustrates the I–V plots of the ICa measured in control hair cells (filled circles) or in the presence of 2 mM glutamate (filled triangles, mean ± SEM, 7 cells). Ca^{2+} currents were elicited by depolarizing voltage pulses (50-ms duration) from −50 mV to +50 mV in 20-mV increments, from a holding potential of −70 mV.

An example of the ICa recorded during a 180-ms voltage ramp from −70 to +40 mV is shown in Fig. 11A, the peak current amplitude was −220 pA in the presence of 2 mM sodium glutamate versus −210 pA in control and the time

courses were superimposable. This experiment was repeated in three cells: the averaged peak amplitudes were −222 ± 73 pA in the presence of 2 mM glutamate versus −230 ± 75 pA in control. This indicates that glutamate did not directly affect the calcium channel biophysical properties and consequently did not modify Ca^{2+} entry into the hair cell. A full I–V curve was measured in 7 cells, by stepping from a −70 mV holding potential to −50, −30, −10, +10, +30 or +50 mV command potentials; the results, displayed in Fig. 11B, confirm that glutamate does not affect ICas in the hair cell. These measurements rule out possible actions of glutamate on Ca conductances in the hair cell, whether basal or ligand activated or voltage-dependent.

As regards the potassium conductances, the compound delayed potassium current, IKD, was examined in particular. This conductance is voltage-dependent (a fraction, IKCa, also is calcium-dependent); in hair cells it is therefore continuously modulated by the receptor potential and its main role is to promote hair cell repolarization, thus controlling transmitter release (Martini et al., 2009, 2013, 2015; Rossi et al., 2017). IKD was evoked in response to command potential values of −40, −20, 0 and +40 mV, from a −70 mV holding potential. IKD amplitude was systematically reduced by glutamate at all values of command potential in all cells (Wilcoxon's signed rank test) both in the range −40 to 0 mV ($W(12) = -78$, $\%\Delta = -39.7$ to −16.8%, $\Delta = -21.7$ to −60.4 pA, $\rho^2 = 1/1$, $P \leq 0.001$) and at +40 mV ($W(12) = -58$, $\%\Delta = -12.2\%$, $\Delta = -76$ pA, $\rho^2 = 0.84$, $P \leq 0.05$). In particular, the average decreases were by 38.7% at −40 mV, by 18.2% at −20 mV, by 14.7% at 0 mV and by 8.5% at +40 mV. The systematic decrease in IKD produced by glutamate is graphically illustrated in Fig. 12A.

On the contrary, the mGluRs-II/III inverse agonist LY341495 systematically increased the amplitude of evoked IKD, in all cells tested (Wilcoxon's signed rank test, $W(6) = 21$, $\rho^2 = 1$, $P \leq 0.05$, at all values of command potential (Fig. 12, B): the average increases were by 27.2% at −40 mV, 11.0% at −20 mV, 11.3% at 0 mV and 12.9% at +40 mV.

Examples of the effects of 2 mM glutamate and of 0.5 μM LY341495 on the size of the IKD, evoked in two different hair cells, are illustrated in Fig. 13B, D, respectively. For each cell, only three representative tracings (−20, 0, +40 mV) are shown for clarity.

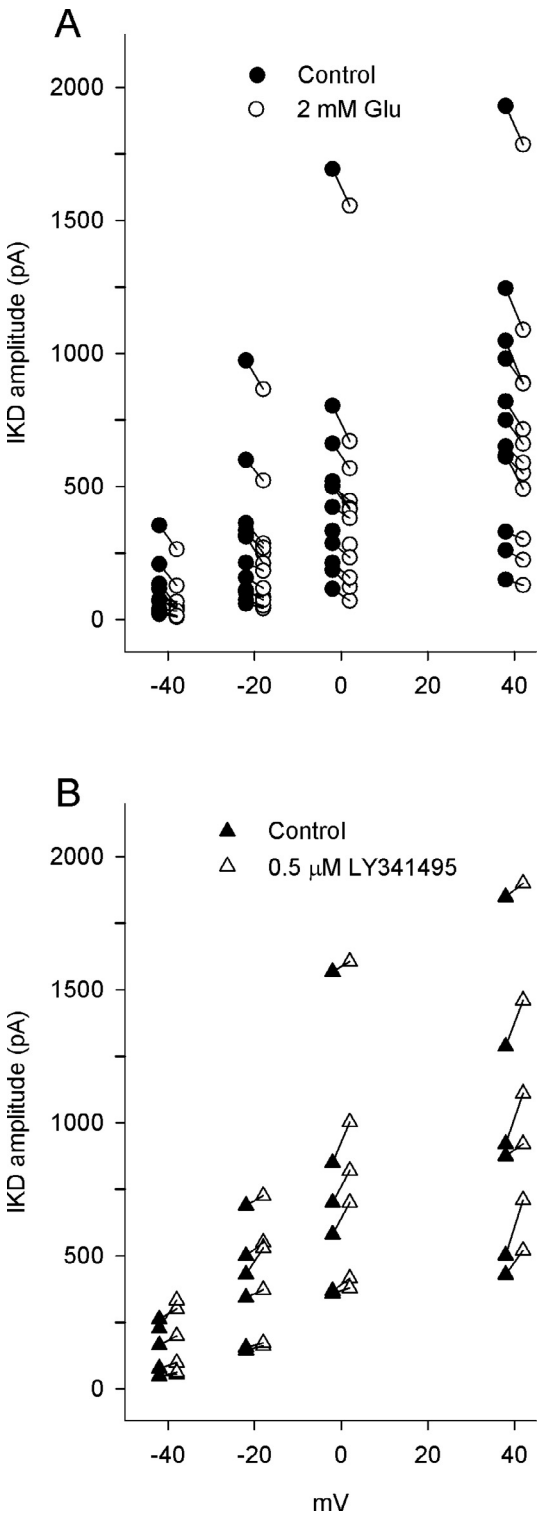

Fig. 12. The effect of sodium glutamate or LY341495 on IKD. Panel (A) compares IKD values in control (filled circles) and in the presence of 2 mM glutamate (empty circles) in 12 units. Panel (B) compares IKD values in control (filled triangles) and in the presence of 0.5 μM LY341495 (empty triangles) in seven different units. In both panels, IKD was evoked by voltage-steps in the range −40 to +40 mV, from −70 mV holding potential.

DISCUSSION

Postsynaptic effect of glutamate and glutamate receptor antagonists

Our results indicate that the application of 5 mM glutamate to the frog isolated and intact labyrinth significantly increases resting and mechanically evoked mEPSP and spike frequency in the afferent fibers from the semicircular canal, without modifying the single mEPSP parameters.

The present results are in line with those previously reported by Prigioni and Russo (1995), who tested the effects of ionophoretically applied glutamate on the spontaneous discharge, and with the facilitation of the resting and evoked synaptic activity reported in the

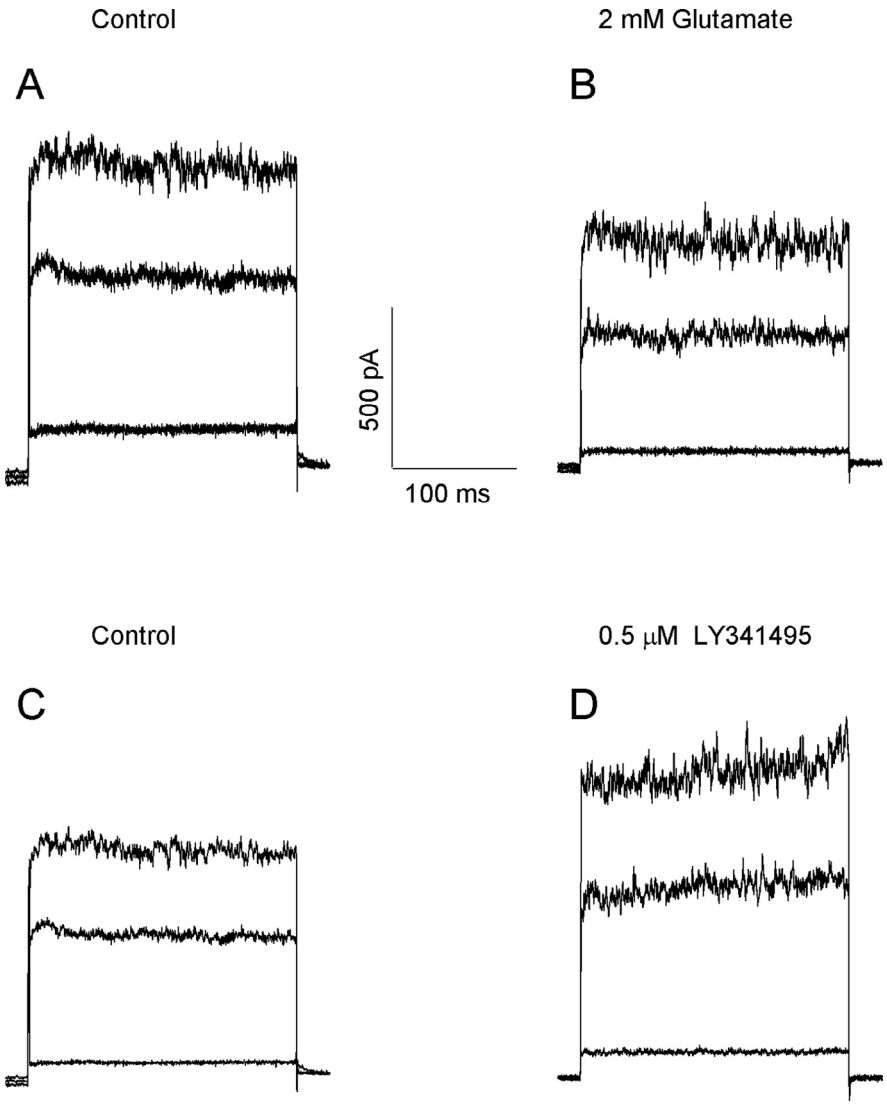

Fig. 13. Examples of current tracings that show the effects of glutamate or LY341495 on IKD. Panels (A) and (B) compare IKD recorded at −20, 0 or +40 mV from an isolated hair cell in control (A) or after applying 2 mM glutamate (B). Panels (C) and (D) similarly compare IKD recorded from another hair cell in control (C) or after 0.5 μM LY341495 (D).

presence of mGluR-I agonists, such as ACPD (Guth et al., 1998b) or DHPG (Hendricson and Guth, 2002a; Rossi et al., 2006).

Although AMPA receptors have been found in the frog semicircular canal, (Prigioni and Russo, 1995; see Guth et al., 1998a for a review), little is known about the precise subtype composition of labyrinthine AMPA receptors. A detailed paper came out recently (Sebe et al., 2017), showing that GluA2, GluA3 and GluA4 subunits are expressed at auditory afferent terminals, and that Ca^{2+}-permeable AMPAR subunits (rather than a NMDAR) may be involved in excitotoxicity produced by loud sounds in auditory hair cells; however the relevance of this to our preparation is uncertain.

Our experiments confirm that AMPA receptors are involved; in fact mEPSP sizes were significantly decreased by low doses of CNQX, whereas D-AP5, a specific blocker of NMDA-Rs, did not affect mEPSP peak amplitude at concentrations up to 100 μM. Since no effects were observed after applying Mg-free Ringer solution and/or glycine (up to 50 μM), with or without D-AP5, we conclude that NMDA-Rs are very unlikely to be involved.

Similar results have been reported in the isolated rat cochlea by Glowatzki et al. (2006); in those experiments, 10 μM CNQX were sufficient to completely block EPSCs in the afferent fibers; the higher sensitivity in that preparation might be due to a drug sensitivity higher than in the intact labyrinth, or to different GluR subtypes or density in the two preparations, or to different degrees of convergence on auditory nerve fibers (one-to one connections in mammalian cochlea vs. an estimated convergence of 6–7 hair cells on a single afferent fiber, according to data from Taglietti et al., 1973; Russo et al., 2007).

Results similar to those obtained by applying exogenous glutamate were observed when glutamate clearance was impaired by the application of DL-TBOA, a broad-spectrum glutamate transporter antagonist (Shimamoto et al., 1998).

The exact nature and functioning of glutamate clearance in frog labyrinthine organs is not clear.

Efficient mechanisms to remove glutamate from the extracellular space are known to be present at most glutamatergic synapses, to avoid receptor desensitization and/or excitotoxicity.

In mammalian cochlea, glutamate–aspartate transporter GLAST (EAAT1) mediates glutamate uptake at the inner ear hair cell afferent synapses: synaptically released glutamate diffuses to supporting cells, where it binds to GLAST and is moved intracellularly (Glowatzki et al., 2006). This is a further function of supporting cells, in addition to their roles in spiral ganglion neuron development and survival (Zilberstein et al., 2012), and in the development, function, survival, death, phagocytosis and regeneration of other cell types within the inner ear; thus, these cells display roles similar to those described for glial cells in other parts of the nervous system (see Monzack and Cunningham, 2013 for a review). Astrocyte-like cells, such as inner phalangeal cells and border cells located near inner hair cell afferent synapses, also exhibit immunoreactivity to GLAST (Furness and Lehre, 1997; Hakuba et al., 2000; Furness and Lawton, 2003) and GLAST-deficient mice have exhibited impaired recovery from acoustic overstimulation

(Hakuba et al., 2000), suggesting an important role for this transporter in preventing glutamate accumulation. Both glutamine synthetase and GLAST (needed to support the glutamate–glutamine cycle, i.e. to uptake glutamate and supply back glutamine to the presynapse) have been shown to be expressed in the supporting cells of the rat vestibular end organ using immunocytochemical techniques and confocal microscopy (Takumi et al., 1997).

In disagreement with our results, Graydon et al. (2014) have shown that DL-TBOA had no effect at the frog amphibian papilla, a sound-detecting organ. In that system large, open regions of extracellular space surround the specialized spine-like contacts between individual afferent fibers and hair cells; this would speed-up transmitter clearance and reduce glutamate spillover between neighboring synapses, suggesting that transmitter diffusion and dilution, rather than uptake, provide efficient clearance of the transmitter at those particular synapses.

In the inner ear, AMPA receptors are usually considered prone to desensitization in the persistent presence of relevant concentrations of glutamate (see, e.g., Ruel et al., 1999). The lack of effects of bath-applied glutamate, or uptake block by DL-TBOA, on mEPSP size indicates that these procedures do not produce remarkable desensitization of the involved post-junctional receptors.

This result is consistent with the observations reported by Glowatzky et al. (2006) in mouse cochlea and by Schnee et al. (2013) in the turtle auditory afferent fibers: no desensitization of AMPA receptors ensued during long-lasting recordings of EPSCs in the presence of steady high external potassium concentration (up to 40 mM). In our preparation, in particular, desensitization must be tightly controlled, since the afferent synapse continuously releases glutamate at rest (in some fibers mEPSP resting frequency exceeds 250 event/s). During excitatory stimulation the peak frequency may rise up to 800 event/s, and still the impaled fiber faithfully transmits the sensory information during long stimulation periods (> 30 s) and maintains this capability when the stimulation is repeated several times (for example see Rossi et al., 2017).

Pre-junctional effects of glutamate

The observed enhancement of synaptic activity by exogenous glutamate and by DL-TBOA points to an action of the transmitter on the hair cell itself.

Ionotropic and/or mGluRs might mediate these actions. A presynaptic ionotropic effect can be excluded, since glutamate application to resting hair cells (membrane potential held to −40, −70 or −100 mV) did not activate any conductance. The mGluRs constitute a group of G protein-coupled receptors (GPCRs) comprised of eight subtypes that are divided into three subgroups based on sequence homology, G protein-coupling specificity, and ligand-binding profiles (see Niswender and Conn, 2010 for a review).

Type I mGluRs have been shown to be expressed by hair cells in the frog semicircular canal (Guth et al., 1998b); they are coupled to G_q which induces Ca^{2+} release from intracellular stores and may therefore account for the ability of glutamate to enhance transmitter release. Activation of these receptors by the mGluR agonist ACPD increases afferent firing at the intact posterior canal. This effect is absent if synaptic transmission is impaired by reducing extracellular Ca^{2+} and is blocked by mGluR antagonists 4-CPG and AIDA (Guth et al., 1998b). It is of interest that these blockers have no effect on their own, suggesting that the mGluRs-I are only relevant when the junction is stimulated (Guth et al., 1998b). In the experiments presented here all drugs tested increased both the resting activity and the evoked response. A type I mGluR on the hair cell (i.e. an autoreceptor) might mediate a positive feedback on transmitter release, via IP_3 (and possibly ryanodine) receptors on the ER (Lelli et al., 2003; Rossi et al., 2006). Actually, Li et al. (2001) did show that glutamate induces a modulation of free Ca^{2+} through release from the ER in isolated inner hair cells of the guinea pig cochlea.

Calcium mobilization from the intracellular stores may contribute to explain why a symmetric mechanical stimulation of the semicircular canal produces an overall increase in mean quantal release, to the point that the rates of synaptic discharge during the inhibitory phase of simulation often are comparable to the resting rates; this phenomenon, which has been observed under most experimental conditions, was previously suggested to be possibly due to the persistence of calcium inflow during the inhibitory phase of the sinusoidal stimulus (Martini et al., 2015).

The effects here reported for LY341495, a blocker or inverse agonist of mGluRs-II/III, suggest that hair cells also express this subtype. Type II/III mGluRs are coupled to $G_{i/0}$ and have been shown to depress glutamate release in several regions of the CNS, through a variety of mechanism such as inhibition of voltage-gated calcium channels (presumably by the $\beta\gamma$ subunit), interference with vesicle fusion and release machinery (presumably by reducing protein phosphorylation by PKA) and activation of presynaptic potassium channels (presumably by direct action of $\alpha_{i/0}$) (see Johnson and Lovinger, 2016 for a review).

A number of quite specific drugs are now available to target these receptors (mGluRs-II and mGluRs-III; see Niswender and Conn, 2010 for a review): among others, LY379268, an agonist of metabotropic mGluRs-II/III, and LY341495, an antagonist or inverse agonist. To our knowledge, neither drug had been tested in auditory or vestibular systems up to now. Cahusac and Senaok (2006) described an enhancement of the response of slowly adapting type I mechanoreceptors by high LY341495 concentration (100 μM); however, this drug concentration most likely blocked all kinds of mGluRs.

In the intact labyrinth, the mGluR-II/III agonist LY379268 did not produce any effect, suggesting that the glutamate levels present in our preparation may already activate this receptor to a significant extent. Conversely, the mGluRs-II/III blocker (or inverse agonist) LY341495 displayed a strong facilitatory action on transmitter release.

According to Tocris, the two drugs employed here to affect mGluR-II/III have different specificity, LY379268 being a specific agonist of mGluR-II (mGlu2 and mGlu3),

whereas LY341495 is an antagonist of the same receptor subtypes but also binds, although with lower affinity, to mGlu8, mGlu7a, mGlu1a (K_i ~7 μM in humans), mGlu5a and mGlu4a. The lack of effects of the agonist, as opposed to a clearly detectable effect of the antagonist on both IKD and transmitter release, may be due either to a high basal activation of the receptor, by glutamate present in the intact and working preparation, or to the fact that the specific subtype expressed by the hair cell is a receptor other than mGlu2 or mGlu3, possibly sensitive to LY341495 but not to LY379268.

The facilitatory effect of LY341495 implies that mGluR-II/III are activated to a significant degree in basal conditions and suggests that these receptors exert a tonic autoinhibitory control on glutamate release from hair cells, as described for synapses in the CNS (Howson and Jane, 2003). Under these conditions LY341495 appears to behave as an inverse agonist, in agreement with observations in rat cortical slices (Fribourg et al., 2011). Since mGluRs-II/III are coupled to $G_{i/0}$, inverse agonism on this receptor is expected to favor substrate phosphorylation, which may enhance the transmitter release machinery (Rossi et al., 2017).

In order to further clarify the possible mechanisms of pre-junctional actions of glutamate, patch-clamp recordings have been performed in isolated hair cells, to investigate whether any bioelectric effects could be involved. The lack of effects of glutamate on the ICas excludes a direct effect of the transmitter on voltage-dependent calcium channels. Enhancement of transmitter release is therefore more likely produced by calcium release from intracellular stores, a process that has been shown to be relevant in semicircular canal hair cells (Lelli et al., 2003; Rossi et al., 2006); as mentioned, this would presumably occur through activation of mGluRs-I.

On the other hand, potassium currents are clearly affected by both glutamate and the mGluRs-II/III inverse agonist LY341495. Since this receptor is coupled to $G_{i/0}$, glutamate is expected to reduce PKA-dependent phosphorylation of substrates in the vicinity of the receptors; this would explain the decreased responsiveness of IKD conductances, which have been shown to require PKA-dependent phosphorylation to effectively recover from inactivation (Martini et al., 2013; Rossi et al., 2017).

The functional consequences of PKA activation in hair cells are quite complex: phosphorylation of IKD would enhance hair cell repolarizing power and should decrease transmitter release, in principle, but phosphorylation processes have been proposed to be important also in sustaining transmitter release (Rossi et al., 2017). The release of Ca^{2+} from the ER, produced by activation of mGluR-I by glutamate, is likely to prevail on these processes producing an overall increase in transmitter release. On the other hand, LY341495, by blocking mGluRs-II/III and favoring PKA-dependent phosphorylation, would simultaneously enhance both the hair cell repolarizing power and the transmitter release process; the latter effect appears to prevail, producing a facilitatory effect on the afferent discharge.

In conclusion, glutamate appears to exert a complex feedback action on the vestibular hair cell, at the frog semicircular canal: on the one hand it enhances Ca^{2+} responses by activating the phospholipase-C/IP_3 path through mGluRs-I; on the other hand, it moderates the activity of the secretory machinery by interfering with substrate phosphorylation, through the $G_{i/0}$-coupled mGluRs-II/III.

The overall action of glutamate at the cytoneural junction

The data here reported confirm that glutamate is the transmitter at the labyrinthine cytoneural junction; experiments with the antagonists indicate that AMPA, but not NMDA, receptors are involved. The post-junctional receptors appear to be scarcely affected by desensitization, although mEPSP size did finally decline in prolonged experiments (> 6 min) under conditions of increased junctional activity and in the presence of exogenous glutamate.

All our experiments point to relevant actions of glutamate on the hair cell itself. Administration of exogenous glutamate markedly increased transmitter release. So did inhibition of glutamate reuptake. Activation of mGluRs-I, which are expressed by these hair cells (Guth et al., 1998b), is the likely mechanism. This would constitute a positive feedback mechanism that might be relevant in determining the dynamics of transmitter release at the vestibular cytoneural junction, by regulating intracellular Ca^{2+} distribution and dynamics.

On the other hand, the strong enhancement of transmitter release by mGluRs-II/III blocker LY341495 indicates that these receptors also are expressed by the hair cell, and that they are constitutively active in the intact preparation. This may constitute a counter-balancing negative feedback mechanism, based on the regulation of phosphorylation processes.

The effects here reported for glutamate on the hair cell may be important to shape the response of the semicircular canal so that information about head angular velocity reaches the central nervous system. Given the hydrodynamic properties of the cupula-endolymph system, the cilia are displaced by angular acceleration, with some delay; a positive feedback loop mediated by GluR-I receptors, acting through a slightly delayed rise in intracellular Ca^{2+}, would help sustaining transmitter release and setting it almost in phase with head velocity. A similar effect is brought about by impaired phosphorylation of IKD, mediated by mGluR-II/III, which reduces the repolarizing power of the hair cell.

A second important consequence of the presynaptic effects here reported is that the amount of transmitter released during a full cycle of mechanical sinusoidal rotation – during which the cilia are displaced to the same extent in the excitatory and inhibitory directions – is expected to be larger than at rest; this was consistently observed in our studies. If mGluRs are expressed by cochlear hair cells (e.g. Kleinlogel et al., 1999), a similar mechanism may be crucial there in order to enhance transmitter release when the cilia vibrate at

such a speed (up to 20 kHz) that the position of the cilia cannot modulate release in real time.

ACKNOWLEDGMENTS

We thank Prof. Oscar Sacchi for his helpful comments on our manuscript and Dr. Angela Pignatelli for her support in program implementation. This work was supported by local funds from the Ferrara University to M. L. R.

REFERENCES

Annoni JM, Cochran SL, Precht W (1984) Pharmacology of the vestibular hair cell-afferent fiber synapse in the frog. J Neurosci 4:2106–2116.

Bonsacquet J, Brugeaud A, Compan V, Desmadryl G, Chabbert C (2006) AMPA type glutamate receptor mediates neurotransmission at turtle vestibular calyx synapse. J Physiol 576:63–71. https://doi.org/10.1113/jphysiol.2006.116467.

Cahusac PM, Senaok SS (2006) Metabotropic glutamate receptor antagonists selectively enhance responses of slowly adapting type I mechanoreceptors. Synapse 59:235–242. https://doi.org/10.1002/syn.20236.

Dechesne C, Raymond J, Sans A (1984) Action of glutamate in the cat labyrinth. Ann Otol Rhinol Laryngol 93. 163–155.

Demêmes D, Lleixa A, Dechesne CJ (1995) Cellular and subcellular localization of AMPA-selective glutamate receptors in the mammalian peripheral vestibular system. Brain Res 67:83–94.

Devau G, Lehouelleur J, Sans A (1993) Glutamate receptors on type I vestibular hair cells of guinea-pig. Eur J Neurosci 5:1210–1217.

Fribourg M, Moreno JL, Holloway T, Provasi D, Baki L, Mahajan R, Park G, Adney SK, Hatcher C, Eltit JM, Ruta JD, Albizu L, Li Z, Umali A, Shim L, Fabiato A, MacKerell Jr AD, Brezina V, Sealfon SC, Filizola M, González-Maeso J, Logothetis DE (2011) Decoding the signaling of a GPCR heteromeric complex reveals a unifying mechanism of action of antipsychotic drugs. Cell 147:1011–1023. https://doi.org/10.1016/j.cell.2011.09.055.

Furness DN, Lawton DM (2003) Comparative distribution of glutamate transporters and receptors in relation to afferent innervation density in the mammalian cochlea. J Neurosci 23:11,296–11,304.

Furness DN, Lehre KP (1997) Immunocytochemical localization of a high-affinity glutamate-aspartate transporter, GLAST, in the rat and guinea-pig cochlea. Eur J Neurosci 9:1961–1969.

Glowatzki E, Cheng N, Hiel H, Yi E, Tanaka K, Ellis-Davies GC, Rothstein JD, Bergles DE (2006) The glutamate-aspartate transporter GLAST mediates glutamate uptake at the inner hair cell afferent synapses in the mammalian cochlea. J Neurosci 26:7659–7664. https://doi.org/10.1523/JNEUROSCI.1545-06.2006.

Graydon CW, Cho S, Diamond JS, Kachar B, von Gersdorff H, Grimes WN (2014) Specialized postsynaptic morphology enhances neurotransmitter dilution and high-frequency signaling at an auditory synapse. J Neurosci 34:8358–8372. https://doi.org/10.1523/JNEUROSCI.4493-13.2014.

Guth PS, Perin P, Norris CH, Valli P (1998a) The vestibular hair cells: post-transductional signal processing. Prog Neurobiol 54:193–247.

Guth PS, Holt JC, Perin P, Athas G, Garcia M, Puri A, Zucca G, Botta L, Valli P (1998b) The metabotropic glutamate receptors of the vestibular organs. Hear Res 125:154–162.

Hakuba N, Koga K, Gyo K, Usami SI, Tanaka K (2000) Exacerbation of noise-induced hearing loss in mice lacking the glutamate transporter GLAST. J Neurosci 20:8750–8753.

Hendricson AW, Guth PS (2002a) Transmitter release from *Rana pipiens* vestibular hair cells via mGluRs: a role for intracellular Ca^{++} release. Hear Res 172:99–109.

Hendricson AW, Guth PS (2002b) Signal discrimination in the semicircular canals: a role for group I metabotropic glutamate receptors. Neuroreport 13:1765–1768.

Holt JC, Xue J-T, Brichta AM, Goldberg JM (2006) Transmission between type II hair cells and bouton afferents in the turtle posterior crista. J Neurophysiol 95:428–452. https://doi.org/10.1152/jn.00447.2005.

Holt JC, Chatlani S, Lysakowski A, Goldberg JM (2007) Quantal and nonquantal transmission in calyx-bearing fibers of the turtle posterior crista. J Neurophysiol 98:1083–1101. https://doi.org/10.1152/jn.00332.2007.

Howson PA, Jane DE (2003) Actions of LY341495 on metabotropic glutamate receptor mediated responses in the neonatal rat spinal cord. British J Pharmacol 139:147–155.

Johnson KA, Lovinger DM (2016) Presynaptic G protein-coupled receptors: gatekeepers of addiction? Front Cell Neurosci 10:264. https://doi.org/10.3389/fncel.2016.00264.

Kleinlogel S, Oestreicher E, Arnold T, Ehrenberger K, Felix D (1999) Metabotropic glutamate receptors group I are involved in cochlear neurotransmission. Neuroreport 10:1879–1882.

Lelli A, Perin P, Martini M, Ciubotaru CD, Prigioni I, Valli P, Rossi ML, Mammano F (2003) Presynaptic calcium stores modulate afferent release in vestibular hair cells. J Neurosci 23:6894–6903.

Li X, Sun J, Yu N, Sun Y, Tan Z, Jiang S, Li N, Zhou C (2001) Glutamate induced modulation of free Ca(2+) in isolated inner hair cells of the guinea pig cochlea. Hear Res 161:29–34.

Lysakowski A, Gaboyard-Niay S, Calin-Jageman I, Chatlani S, Price SD, Eatock RA (2011) Molecular microdomains in a sensory terminal, the vestibular calyx ending. J Neurosci 31:10101–10114. https://doi.org/10.1523/JNEUROSCI.0521-11.2011.

Martini M, Rossi ML, Rubbini G, Rispoli G (2000) Calcium currents in hair cells isolated from semicircular canals of the frog. Biophys J 78:1240–1254.

Martini M, Farinelli F, Rossi ML, Rispoli G (2007) Ca^{2+} current of frog vestibular hair cells is modulated by intracellular ATP but not by long-lasting depolarisations. Eur Biophys J 36:779–786. https://doi.org/10.1007/s00249-007-0172-0.

Martini M, Canella R, Fesce R, Rossi ML (2009) Isolation and possible role of fast and slow potassium current components in hair cells dissociated from frog crista ampullaris. Pflügers Arch 457:1327–1342. https://doi.org/10.1007/s00424-008-0598-y.

Martini M, Canella R, Fesce R, Rossi ML (2013) The amplitude and inactivation properties of the delayed potassium currents are regulated by protein kinase activity in hair cells of the frog semicircular canals. PLoS One 8. https://doi.org/10.1371/journal.pone.0067784 e67784.

Martini M, Canella R, Rubbini G, Fesce R, Rossi ML (2015) Sensory transduction at the frog semicircular canal: how hair cell membrane potential controls junctional transmission. Front Cell Neurosci. https://doi.org/10.3389/fncel.2015.00235.

Monzack EL, Cunningham LL (2013) Lead roles for supporting actors: critical functions of inner ear supporting cells. Hear Res 303:20–29. https://doi.org/10.1016/j.heares.2013.01.008.

Niedzielski AS, Safieddine S, Wenthold RJ (1997) Molecular analysis of excitatory amino acid receptor expression in the cochlea. Audiol Neurootol 2:79–91.

Niswender CM, Conn PJ (2010) Metabotropic glutamate receptors: physiology, pharmacology, and disease. Annu Rev Pharmacol Toxicol 50:295–322. https://doi.org/10.1146/annurev.pharmtox.011008.145533.

Ottersen OP, Takumi Y, Matsubara A, Landsend AS, Laake JH, Usami S-I (1998) Molecular organization of a type of peripheral glutamate synapse: the afferent synapses of hair cells in the inner ear. Prog Neurobiol 54:127–148.

Prigioni I, Russo G (1995) Glutamate excitatory effects on ampullar receptors of the frog. Amino Acids 9:265–273. https://doi.org/10.1007/BF00805957.

Prigioni I, Russo G, Masetto S (1994) Non-NMDA receptors mediate glutamate-induced depolarization in frog crista ampullaris. Neuroreport 5:516–518.

Raymond J, Dememes D, Nieoullon A (1988) Neurotransmitters in vestibular pathways. Prog Brain Res 76:29–43.

Rossi ML, Martini M, Pelucchi B, Fesce R (1994) The quantal nature of transmitter release at the cytoneural junction of the frog labyrinth. J Physiol 478:17–35.

Rossi ML, Prigioni I, Gioglio L, Rubbini G, Russo G, Martini M, Farinelli F, Rispoli G, Fesce R (2006) IP3 receptor in the hair cells of frog semicircular canal and its possible functional role. Eur J Neurosci 23:1775–1783. https://doi.org/10.1111/j.1460-9568.2006.04708.x.

Rossi ML, Rubbini G, Gioglio L, Martini M, Fesce R (2010) Exposure to reduced gravity impairs junctional transmission at the semicircular canal in the frog labyrinth. Am J Physiol Regul Integr Comp Physiol 298:R439–R452. https://doi.org/10.1152/ajpregu.00673.2009.

Rossi ML, Rubbini G, Martini M, Canella R, Fesce R (2017) Forskolin and protein kinase inhibitors differentially affect hair cell potassium currents and transmitter release at the cytoneural junction in the isolated frog labyrinth. Neuroscience 357:20–36. https://doi.org/10.1016/j.neuroscience.2017.05.039.

Ruel J, Chen C, Pujol R, Bobbin RP, Puel JL (1999) AMPA-preferring glutamate receptors in cochlear physiology of adult guinea-pig. J Physiol 518:667–680.

Russo G, Calzi D, Martini M, Rossi ML, Fesce R, Prigioni I (2007) Potassium currents in the hair cells of vestibular epithelium: position-dependent expression of two types of A channels. Eur J Neurosci 25:695–704. https://doi.org/10.1111/j.1460-9568.2007.05327.x.

Sadeghi SG, Pyott SJ, Yu Z, Glowatzki E (2014) Glutamatergic signaling at the vestibular hair cell calyx synapse. J Neurosci 34:14,536–14,550. https://doi.org/10.1523/JNEUROSCI.0369-13.2014.

Safieddine S, Wenthold RJ (1997) The glutamate receptor subunit delta1 is highly expressed in hair cells of the auditory and vestibular systems. J Neurosci 17:7523–7531.

Schnee ME, Castellano-Muñoz M, Ricci AJ (2013) Response properties from turtle auditory hair cell afferent fibers suggest spike generation is driven by synchronized release both between and within synapses. J Neurophysiol 110:204–220. https://doi.org/10.1152/jn.00121.2013.

Sebe JY, Cho S, Sheets L, Rutherford MA, von Gersdorff H, Raible DW (2017) Ca2 + -permeable AMPARs mediate glutamatergic transmission and excitotoxic damage at the hair cell ribbon synapse. J Neurosci 37:6162–6175. https://doi.org/10.1523/JNEUROSCI.3644-16.2017.

Shimamoto K, Lebrun B, Yasuda-Kamatani Y, Sakaitani M, Shigeri Y, Yumoto N, Nakashama T (1998) DL-Threo-b-benzyloxyaspartate, a potent blocker of excitatory amino acid transporters. Mol Pharmacol 53:195–201.

Taglietti V, Valli P, Casella C (1973) Discharge properties and innervation of the sensory units in the crista ampullaris. Arch Sci Biol 57:73–86.

Takumi Y, Matsubara A, Danbolt NC, Laake JH, Storm-Mathisen J, et al. (1997) Discrete cellular and subcellular localization of glutamine synthetase and the glutamate transporter GLAST in the rat vestibular end organ. Neuroscience 79:1137–1144.

Usami SI, Takumi Y, Matsubara A, Fujita S, Ottersen OP (2001) Neurotransmission in the vestibular endorgans – glutamatergic transmission in the afferent synapse of hair cells. Biol Sci Space 15:367–370.

Zilberstein Y, Liberman MC, Corfas G (2012) Inner hair cells are not required for survival of spiral ganglion neurons in the adult cochlea. J Neurosci 32:405–410. https://doi.org/10.1523/JNEUROSCI.4678-11.2012.

(Received 13 February 2018, Accepted 8 June 2018)
(Available online 18 June 2018)